THE ASTROPHYSICAL JOURNAL, 273:530–538, 1983 October 15

THE CARINA DWARF SPHEROIDAL—AN INTERMEDIATE AGE GALAXY

JEREMY MOULD[1]
Palomar Observatory, California Institute of Technology
AND
MARC AARONSON[1]
Steward Observatory, University of Arizona
Received 1983 February 28; accepted 1983 March 23

ABSTRACT

Deep B and V frames have been obtained of the Carina dwarf spheroidal galaxy with the CTIO prime focus CCD camera. The resulting color-magnitude diagram reaches $V = 24$ mag, and a main-sequence turnoff is apparent at $V = 23$ mag. A well-defined red horizontal branch yields a distance modulus $(m - M)_0 = 19.8$, along with $[Fe/H] = -1.9 \pm 0.2$ from Sandage's $(B - V)_{0,g}$ calibration. Both isochrone fitting and the horizontal-branch, turnoff difference $\Delta M_{HB-TO} \sim 2.5$ mag yield an age estimate for the bulk of the stellar population of 7.5 ± 1.5 Gyr. A comparison of the Carina luminosity function with theoretical predictions leaves little room for a Population II component in this galaxy. This is consistent with other arguments which suggest that the fraction of old (16 Gyr) stars is small. This makes Carina the leading contender for a galaxy which did not form stars until the universe was old.

Subject headings: galaxies: individual — galaxies: photometry — galaxies: stellar content

I. INTRODUCTION

The Carina galaxy, discovered by Cannon, Hawarden, and Tritton (1977) on SRC Schmidt survey plates, is one of the "dwarf spheroidal" satellites, which, together with the globular clusters, some high velocity field stars, and the Magellanic Clouds, constitute the remote halo of the Milky Way. Although canonical models for the formation of the Milky Way postulate that stars in the outer halo are among the oldest in the Galaxy, carbon stars were discovered in the Carina dwarf (Cannon, Niss, and Norgaard-Nielsen 1981) and seem to be a common feature of dwarf spheroidals (see the reviews by Mould [1982] and Aaronson, Olszewski, and Hodge [1983]). Comparison of these stars with those of globular clusters in the Magellanic Clouds suggested to Mould *et al.* (1982) that Carina might consist substantially of an intermediate-age stellar population.

A clear test of the latter hypothesis is available by examination of the main-sequence turnoff of the Carina galaxy. The results of such an investigation are reported in this paper.

II. IMAGING AND PHOTOMETRY

CCD images of suitable fields in the neighborhood of the Carina dwarf galaxy were obtained with the KPNO CCD system at the prime focus of the 4 m telescope at Cerro Tololo. The observations were made during the dark hours of three nights in November 1982, as logged in Table 1. The Carina fields are offset approximately 5′ west of SAO 234657; the small additional offset for Carina 2 eliminated the mild intrusion of scattered light from this star into the Carina 1 frames. A control field was observed 1° south of Carina (at the same galactic latitude) to determine the effects of foreground and background objects.

Flat-field calibration frames were prepared by observation of an illuminated screen on the 4 m dome and corrected for 1% gradients by means of median-filtered, stepped exposures on dark blank sky. Changes in the flat-field response were tested for, but not detected, and the same calibration frames were used for all three nights. The data frames were bias corrected and then divided by these flat-field calibration frames, and the set of longer observations was averaged after quantitative tests for similarity. No correction was made to the data frames for dark current or "bad" pixels. The final processing step was subtraction of the scaled AC component of the processed blank sky from the V frames to remove the effect of λ5577 induced fringes in the sky background. Through careful scaling such fringing could be completely removed.

Standards were observed under photometric conditions in the E2 and E3 regions and the NGC 300 field (Graham 1981, 1982). Digital aperture photometry using

[1]Visiting Astronomer, Cerro Tololo Inter-American Observatory. CTIO is operated by AURA, Inc., under contract to the National Science Foundation.

TABLE 1

JOURNAL OF CARINA OBSERVATIONS

DATE (UT) 1982	FIELD	POSITION (1950) R.A.	decl.	EXPOSURE TIMES (secs) B	V	B	V	SKY CONDITION	SEEING (FWHM)
Nov 21	Carina 1	$6^h39^m47^s$	−50°56′34″	1×100	1×50	3×1000	5×500	Photometric	1″.3
Nov 22	Control	6 40 53	−51 56 51	1×100	1×50	2×1000	5×500	Photometric	2
Nov 23	Carina 2	6 39 39	−50 56 46	1×90	1×50	3×900	6×500	Light cirrus	1.5
Nov 23	Control	6 40 53	−51 56 51	1×100	1×50	2×1000	2×500	Light cirrus	1.5

8 to 9 arcsec apertures, which include more than 99% of the total starlight, was extinction-corrected with mean coefficients to a b', v' system and fitted to the color equations:

$$V = v' + \text{constant}$$

$$B - V = 1.082(b - v)' + \text{constant}.$$

The color terms in these equations were determined to an accuracy of 2% by Da Costa and Mould (1983) earlier in the same observing run. The formal uncertainty in the constants on November 21, when nine standard stars were measured, was 0.006 mag in V and 0.003 mag in $B - V$.

Similar measurements on 10 bright, uncrowded stars in Carina yielded colors and magnitudes for secondary standards in the Carina 1 field. These results are listed in Table 2 and the stars are identified in Figure 1 (Plates 26–28). The same procedure was followed in the control field (see Table 3).

Faint photometry in these fields was then carried out with the same digital aperture photometry code[2] using a measuring aperture of radius two pixels. All stars visible as unblended images on the blue frame and unaffected by bad pixels or edge effects were identified by hand for photometry. The 10 stars of Table 2 were then used to determine corrections of 0.443 ± 0.006 mag and 0.121 ± 0.002 mag in V and $B - V$ to put measurements of Carina 1 on the b', v' instrumental system. For Carina 2 measurements of 23 stars brighter than $V = 22$ were compared with measurements in Carina 1. Zero point differences were thus determined to a precision comparable to that quoted above. These measurements, which include 122 stars as averages from Carina 1 and 2, are transformed to the standard (B, V) system in Table 4. Table 4 gives an identifying number (col. [1]) (see also Fig. 1); pixel coordinates (cols. [2] and [3]); to assist in cases of confusion, V and $B - V$ magnitudes (cols. [4] and [5]); and the range in $B - V$ for repeated measurements (col. [6]). A few stars with $V > 25$ were omitted. The control field was processed in a similar manner (Table 5).

[2]This code was developed by H. R. Butcher. See Adams *et al.* (1980) for a user's description and Seitzer, Da Costa, and Mould (1983) for a discussion of the summation technique and aperture correction methods.

TABLE 2

SECONDARY STANDARDS IN CARINA

Star	x	y	V	$B - V$
A.......	183	233	18.19	1.42
B.......	132	220	19.72	0.90
C.......	48	78	20.27	0.56[a]
D	121	43	17.69	0.79
E.......	199	349	17.76	0.96
F.......	134	456	17.58	0.71
G	110	457	18.49	0.69
H	31	387	17.80	1.28
I	125	187	15.68	1.46
J	145	367	17.85	1.29

[a]There appears to be a problem with the B measurement for this star.

TABLE 3

SECONDARY STANDARDS IN THE CONTROL FIELD

Star	x	y	V	$B - V$
U	14	458	16.42	0.54
V.......	113	384	17.69	
W	57	363	17.67	0.75
X.......	57	179	16.90	0.71
Y.......	23	145	17.50	0.82
Z.......	208	67	17.19	0.77

III. THE COLOR-MAGNITUDE DIAGRAM

The measurements recorded in Tables 4 and 5 are plotted in color-magnitude diagrams for Carina and for the control field in Figures 2 and 3. From a comparison of these diagrams we infer the following (to be amplified below).

1. Carina has a stubby, red horizontal branch (HB) which, by its concentration, clearly stands out from foreground contamination at $V = 20.5$ (see also Cannon *et al.* 1983).

TABLE 4

PHOTOMETRY IN CARINA

#	x	y	V	B-V	
1	12	401	23.65	0.13	
2	5	398	23.25	0.43	
3	81	392	23.84	0.26	
4	31	387	17.79	1.27	
5	118	386	22.13	0.35	
6	7	382	20.55	0.79	
7	71	373	22.64	0.57	
8	85	360	21.47	0.66	
9	56	359	23.11	0.31	
10	118	358	20.53	0.62	.00
11	46	358	20.29	0.78	.01
12	3	353	23.55	0.49	
13	108	352	22.27	0.32	
14	178	351	22.99	0.31	
15	68	351	23.88	-0.04	.15
16	199	349	17.75	0.96	
17	125	348	21.01	0.75	.03
18	151	346	22.65	0.10	
19	169	345	23.05	0.10	
20	108	345	22.71	0.28	
21	86	342	23.75	0.20	.46
22	179	340	19.81	0.87	
23	34	339	22.16	0.36	.01
24	138	338	22.98	0.25	
25	11	336	20.96	1.25	
26	220	334	20.44	0.76	
27	214	334	19.89	0.87	
28	168	329	20.97	0.72	
29	74	328	21.01	1.62	
30	163	325	20.64	1.38	
31	186	325	23.76	0.42	
32	57	323	22.87	0.41	.10
33	92	323	23.08	0.40	.11
34	65	320	21.72	0.24	.00
35	29	320	22.29	0.20	
36	150	319	19.18	0.94	
37	34	318	22.36	0.61	
38	186	317	22.99	0.24	.04
39	101	314	22.64	0.34	.08
40	41	311	20.48	0.58	.01
41	73	308	24.01	-0.04	
42	204	304	23.06	0.21	
43	162	300	24.03	0.24	
44	123	300	20.27	0.68	.03
45	144	299	23.53	0.50	
46	216	298	23.65	0.72	
47	209	295	23.44	0.22	
48	50	295	22.51	0.65	
49	62	293	22.67	0.35	
50	89	292	22.74	0.34	
51	125	292	20.38	0.90	.01
52	24	291	22.01	0.28	.00
53	33	291	20.12	1.52	.02
54	161	290	23.36	0.02	
55	41	290	24.07	0.50	
56	118	289	22.09	0.62	
57	103	289	20.96	0.73	.06

#	x	y	V	B-V	
58	16	287	23.84	0.26	
59	113	284	20.60	0.82	
60	184	283	23.74	0.18	
61	99	281	24.50	-0.44	
62	75	281	23.76	0.62	
63	217	281	20.73	0.75	.04
64	106	280	23.92	0.19	
65	34	279	22.33	0.52	.00
66	170	277	22.15	0.73	.01
67	96	276	23.91	0.07	.13
68	13	276	23.43	0.29	
69	205	276	22.01	0.37	.04
70	220	276	24.29	-0.06	
71	130	275	22.50	0.45	.08
72	163	274	23.98	0.75	.43
73	197	273	19.89	0.82	.01
74	180	272	24.17	0.35	
75	172	272	23.92	0.67	
76	36	271	23.74	0.46	
77	24	271	23.09	0.63	
78	142	269	23.46	0.29	
79	156	269	22.65	0.65	
80	209	269	22.77	0.30	.03
81	205	268	22.50	0.68	.10
82	10	268	20.51	0.67	
83	149	268	20.91	0.71	
84	40	267	23.65	0.56	
85	121	267	20.05	0.59	
86	184	266	22.98	0.20	.18
87	134	266	23.63	0.09	
88	90	265	22.93	0.25	.03
89	201	262	23.56	0.46	
90	182	261	23.55	0.09	
91	31	261	17.15	0.61	
92	193	261	23.58	0.23	
93	21	259	22.09	0.23	
94	131	258	22.22	0.24	.11
95	186	257	22.77	0.15	.01
96	154	255	24.26	-0.16	
97	103	254	21.98	0.70	
98	171	253	23.60	0.15	
99	193	253	20.24	0.70	
100	147	252	20.80	1.60	.00
101	50	251	22.87	0.41	.18
102	165	247	22.55	0.28	.03
103	151	247	23.01	0.34	.10
104	63	246	23.38	0.38	.20
105	128	245	21.99	0.83	.02
106	198	244	24.43	0.13	
107	41	244	23.51	0.37	.27
108	156	242	23.71	0.34	
109	178	242	24.10	0.23	
110	16	242	20.10	0.74	
111	83	242	21.67	0.22	
112	209	242	23.28	0.36	.24
113	228	240	21.32	0.88	
114	9	240	23.20	0.10	

#	x	y	V	B-V	
115	148	240	23.73	0.82	
116	62	238	22.56	0.58	.05
117	90	236	23.33	0.56	
118	164	236	23.87	0.28	.09
119	123	235	22.66	0.87	
120	111	234	22.74	0.24	
121	21	234	23.38	0.36	
122	32	234	22.37	0.69	.07
123	206	233	22.84	0.54	
124	183	233	18.22	1.42	.01
125	129	233	23.91	0.25	.08
126	36	233	23.06	0.31	
127	214	231	24.12	0.06	
128	23	229	23.99	0.09	.40
129	206	228	22.79	0.73	
130	153	228	21.97	0.65	
131	87	228	18.36	1.42	.00
132	191	227	22.95	0.67	
133	143	226	21.79	1.01	.01
134	233	223	20.12	0.73	
135	178	222	23.32	0.16	.18
136	153	221	23.22	0.21	.07
137	132	220	19.70	0.89	.01
138	113	219	22.75	0.30	.07
139	173	218	23.17	0.25	.02
140	121	214	22.26	0.48	.11
141	228	213	22.24	0.71	.08
142	195	212	22.66	0.47	
143	179	210	23.58	0.23	
144	167	209	22.18	0.04	.02
145	217	208	22.44	0.35	.08
146	48	207	23.97	0.44	.57
147	235	206	22.50	0.27	.15
148	84	204	22.14	0.26	.09
149	106	202	20.89	0.94	
150	223	202	19.31	0.80	.03
151	34	200	24.55	0.05	
152	132	199	22.76	0.51	.08
153	230	199	21.87	0.41	.08
154	202	199	19.38	0.93	.02
155	144	198	20.58	0.51	
156	19	197	23.10	1.16	
157	128	197	23.21	0.46	.10
158	161	196	23.09	0.42	.06
159	207	193	23.10	0.09	
160	27	190	23.51	0.30	
161	76	189	23.26	0.25	.10
162	171	188	23.76	0.39	.53
163	89	188	23.69	0.20	.14
164	161	187	23.61	0.22	.04
165	226	187	23.23	0.02	
166	37	187	23.99	0.47	
167	154	186	21.52	0.72	
168	186	184	23.69	0.44	
169	240	184	23.63	0.01	
170	23	183	22.77	0.59	
171	148	183	23.73	0.21	

2. The giant branch is sparse and badly contaminated by field stars. The location of the giant branch at the HB level, however, is well determined at $B - V = 0.78$.

3. A main-sequence turnoff is detected in the vicinity of V magnitude 23.

4. A number of "blue stragglers" are seen at luminosities higher than this turnoff location.

5. Below the level of the HB foreground star and background object contamination is not a serious problem.

For a critical examination of these conclusions we need some firm estimates of the photometric errors. It is clear from the foregoing that formally the photometric zero points in this work are determined to higher accu-

TABLE 4—*Continued*

#	x	y	V	B–V	
172	228	181	23.13	0.20	.12
173	9	180	23.09	0.37	
174	196	178	24.05	0.25	
175	69	177	23.21	0.46	
176	188	177	20.27	0.76	.08
177	80	175	23.63	0.31	.01
178	35	175	24.16	0.22	
179	220	171	20.41	0.70	
180	50	170	22.28	0.35	
181	58	165	22.71	0.42	
182	78	163	23.53	0.08	
183	24	161	23.46	0.26	
184	53	161	20.43	1.65	.06
185	213	159	22.23	0.15	
186	188	159	18.32	0.84	
187	74	158	23.04	0.32	
188	81	157	23.26	0.52	
189	239	155	22.66	0.25	
190	202	154	23.68	0.26	
191	173	151	22.78	0.29	
192	24	151	23.16	0.76	
193	230	150	22.41	0.47	
194	141	149	23.62	0.29	
195	181	148	23.00	0.30	
196	84	148	23.26	0.17	
197	220	148	23.02	0.25	
198	200	148	23.12	0.16	
199	59	146	24.14	−0.07	
200	39	145	22.61	0.40	.08
201	141	142	23.84	0.41	
202	174	141	23.47	0.27	
203	134	136	23.45	0.21	
204	25	135	23.12	0.30	.09
205	80	131	23.42	0.28	.01
206	161	130	23.23	0.08	
207	86	129	23.01	0.17	
208	167	129	22.64	0.47	
209	220	126	23.18	0.39	.28
210	28	126	19.80	0.82	.00
211	189	124	20.14	0.69	
212	201	122	24.57	0.02	
213	110	119	21.93	0.24	.01
214	181	117	20.91	1.13	
215	168	117	24.03	0.41	
216	23	115	20.53	0.68	
217	252	114	19.93	0.86	
218	199	113	20.54	0.58	
219	233	113	23.35	0.42	
220	120	111	22.02	0.53	
221	225	111	20.42	0.67	.04
222	98	110	22.99	0.32	
223	87	110	22.11	1.34	
224	163	108	20.41	0.64	
225	144	108	17.73	1.49	
226	82	107	22.10	0.41	
227	103	106	23.67	0.60	.01
228	190	102	23.47	0.35	

#	x	y	V	(B–V)	
229	111	102	23.54	0.38	
230	249	101	20.44	0.65	
231	53	100	23.18	0.45	.01
232	45	100	22.74	0.25	.10
233	167	98	24.60	0.02	
234	25	94	21.67	0.68	.01
235	129	92	23.02	0.66	
236	142	90	23.66	0.27	.25
237	170	90	22.85	0.25	.06
238	196	87	22.65	0.48	.18
239	36	84	20.38	0.67	.02
240	209	82	21.21	0.27	.01
241	178	82	21.46	−0.01	
242	136	82	22.73	0.56	.06
243	201	82	21.27	0.70	.03
244	98	80	22.75	0.48	
245	120	79	20.26	0.76	
246	186	78	23.61	0.35	
247	216	77	20.71	0.74	.03
248	46	76	20.25	0.70	.00
249	241	73	22.65	0.39	.04
250	120	72	20.48	0.65	
251	175	71	22.67	0.33	.02
252	39	70	20.59	0.55	
253	58	69	23.50	0.12	
254	236	65	21.02	0.73	.01
255	190	64	23.38	0.38	.23
256	207	64	20.50	0.61	.00
257	170	63	23.81	0.04	
258	225	59	23.56	0.44	
259	162	59	23.33	0.12	.14
260	225	59	23.59	0.27	.32
261	60	58	23.81	0.56	
262	82	57	22.18	0.73	.01
263	219	56	23.58	0.10	.21
264	42	54	22.69	0.30	
265	191	53	23.44	0.57	.27
266	85	51	20.53	0.78	.01
267	181	50	22.62	0.27	.02
268	112	50	21.85	1.40	.04
269	207	48	23.51	0.48	.00
270	43	48	23.11	0.16	
271	79	48	22.80	0.60	
272	168	47	24.17	0.19	
273	65	47	22.32	0.25	.01
274	186	46	22.99	0.33	.03
275	224	46	23.11	0.07	.21
276	19	45	23.04	0.26	
277	121	43	17.70	0.79	.01
278	25	43	22.60	0.61	
279	73	40	23.21	0.12	.13
280	153	40	21.94	1.41	.07
281	163	39	22.98	0.28	
282	134	38	22.50	0.17	.07
283	170	38	22.99	0.28	.15
284	265	36	21.31	0.73	
285	197	32	23.24	0.07	

#	x	y	V	(B–V)	
286	169	31	23.72	0.67	
287	216	29	20.54	0.60	.02
288	59	28	22.34	0.31	.02
289	205	27	23.16	0.20	.19
290	163	27	22.64	0.59	
291	154	27	23.23	0.28	.03
292	137	26	20.58	0.67	.01
293	104	25	21.26	1.30	
294	110	25	21.25	0.70	
295	95	20	21.50	0.71	
296	267	18	22.14	0.65	
297	67	17	22.62	1.14	.01
298	225	17	21.27	0.63	
299	150	16	18.53	0.75	
300	188	15	23.45	0.34	
301	195	14	20.49	0.64	.04
302	228	8	20.34	0.42	
303	76	3	22.06	0.76	
304	147	0	23.84	0.41	
305	110	−5	22.91	0.22	
306	31	−6	22.42	0.60	
307	240	−8	23.63	0.23	
308	223	−8	20.54	−0.07	
309	181	−9	20.69	0.53	
310	117	−9	19.52	0.87	
311	232	−9	22.55	0.51	
312	145	−11	23.65	−0.03	
313	223	−15	22.06	0.65	
314	28	−16	23.87	0.08	
315	147	−19	23.57	0.39	
316	194	−21	22.72	0.03	
317	22	−21	20.62	1.48	
318	75	−21	24.33	−0.12	
319	177	−24	23.79	0.05	
320	242	−27	22.54	0.70	
321	217	−28	22.88	0.22	
322	71	−30	22.67	0.30	
323	233	−31	20.46	0.85	
324	168	−31	22.65	0.05	
325	28	−32	21.62	0.75	
326	240	−33	22.38	0.44	
327	149	−37	22.54	0.48	
328	118	−37	18.75	0.72	
329	206	−37	22.59	0.28	
330	133	−39	22.62	0.20	
331	213	−40	20.79	1.14	
332	124	−52	22.92	0.25	
333	235	−53	22.45	0.57	
334	57	−57	18.29	1.02	
335	198	−59	23.90	0.28	
336	208	−61	17.53	0.85	
337	154	−65	20.92	0.69	
338	185	−68	23.12	0.27	
339	198	−69	22.69	0.44	

racy than the astrophysical uncertainties (in the reddening to Carina, for example). We should concern ourselves, however, with possible biases in the photometry and the size and sources of random errors.

To test for a measurement bias in the aperture photometry technique, magnitudes were determined for the same set of stars, using a point-spread–function fitting program developed by one of us for the Caltech VAX image processing computer. Even with scaling radii as small as one pixel (which reduces the background component of the measurements by a factor of 4), the form of the color-magnitude diagram was unchanged in detail.

In a second experiment artificial stars were replicated from the point-spread function with a known luminosity function and added at random locations to the original

1983ApJ...273..530M

TABLE 5

PHOTOMETRY IN THE CONTROL FIELD

#	x	y	V	B-V		#	x	y	V	B-V	
1	101	472	23.54	0.54		39	136	205	23.23	0.72	.04
2	52	447	21.12	1.01		40	197	204	20.30	0.76	.00
3	171	440	22.83	0.44		41	186	202	23.28	0.56	
4	101	440	21.95	0.09		42	68	201	18.68	0.88	.02
5	85	438	22.73	1.14		43	94	198	22.01	1.44	.25
6	151	429	18.59	1.58		44	137	196	21.27	1.42	.12
7	140	428	20.81	0.47		45	105	194	21.66	1.26	
8	63	425	20.32	0.68		46	35	192	22.81	0.77	.02
9	89	424	23.17	0.56	.11	47	186	190	22.98	0.56	.06
10	97	388	19.94	0.45		48	255	187	19.27	1.31	
11	57	388	21.30	1.29	.09	49	79	185	23.16	0.92	.67
12	75	382	23.10	1.01	.27	50	164	180	21.76	1.75	.22
13	108	382	17.71	0.53	.00	51	210	179	23.53	0.42	.36
14	123	379	20.63	1.51	.02	52	52	178	16.91	0.72	.01
15	37	371	21.94	1.62		53	185	175	23.08	0.20	.04
16	52	362	17.66	0.75	.02	54	219	175	22.06	1.04	.04
17	158	337	21.46	1.03		55	180	160	21.91	1.61	.01
18	12	324	23.01	0.92		56	53	151	18.68	1.00	.02
19	79	312	22.72	1.20	.40	57	220	145	18.44	0.72	.01
20	226	305	21.05	1.50	.04	58	106	144	23.43	0.55	
21	142	304	23.05	0.98	.40	59	18	144	17.50	0.83	
22	128	304	23.72	0.30		60	96	142	21.34	1.05	
23	205	301	22.54	0.97	.06	61	164	141	22.39	1.17	
24	23	299	23.23	0.59		62	137	130	21.79	1.50	.05
25	30	296	23.70	0.31		63	82	120	19.62	1.28	.03
26	201	294	22.80	0.42	.09	64	42	117	22.28	0.76	
27	229	276	20.63	1.66		65	91	114	23.20	0.74	
28	218	271	20.80	1.61		66	172	110	21.84	1.66	.04
29	235	267	23.55	0.57	.30	67	129	109	22.09	1.51	.67
30	213	251	19.54	1.45		68	94	89	22.07	0.83	.03
31	135	248	21.40	0.59	.08	69	26	85	20.69	1.14	
32	234	246	21.62	1.45	.00	70	120	82	18.79	1.65	
33	76	241	20.77	1.58		71	66	52	21.47	1.67	.10
34	263	241	19.36	0.97		72	80	43	20.70	0.70	.01
35	231	239	21.70	1.79		73	162	40	22.38	0.97	.15
36	220	230	22.37	0.94		74	117	36	21.17	0.82	
37	39	227	23.37	0.77	.06	75	29	25	20.58	1.41	
38	140	217	21.93	1.54							

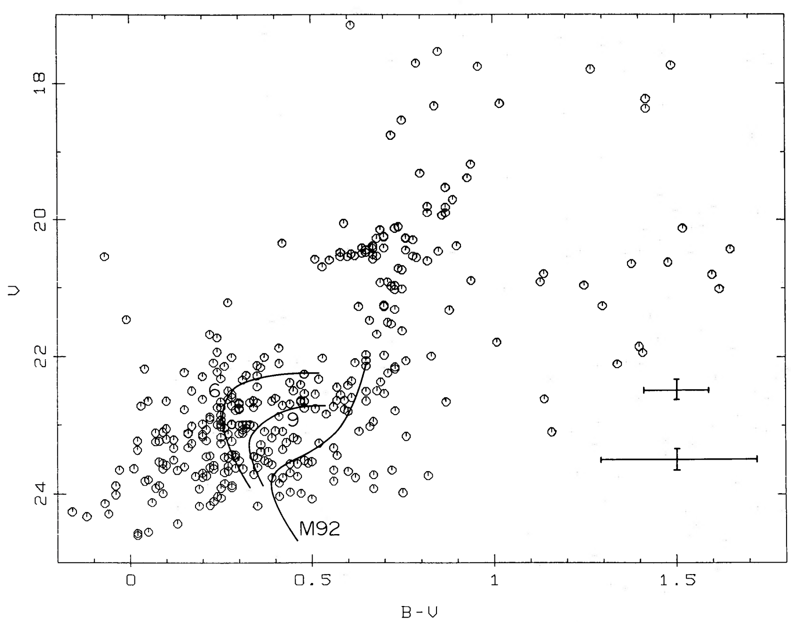

FIG. 2.—The Carina dwarf spheroidal color magnitude diagram. Theoretical isochrones for 6 and 9 Gyrs ($Y = 0.2$, interpolated metallicity) are shown from Ciardullo and Demarque together with Sandage's mean locus of the main sequence for the galactic globular cluster M92. The error bars indicate 1 σ uncertainties for a single star at the corresponding magnitude.

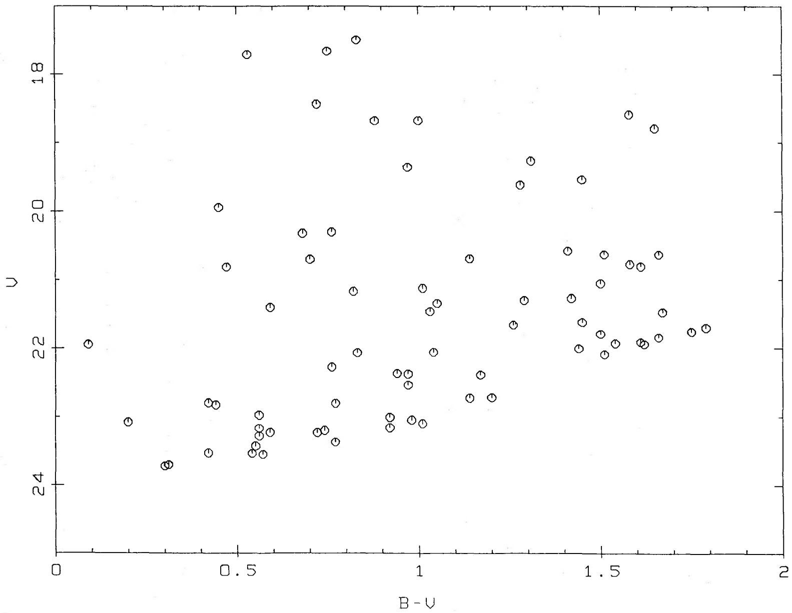

FIG. 3.—Color magnitude diagram of the Carina control field, 1 degree south of the galaxy

TABLE 6

MEASURING ERRORS ANALYSIS

$\delta(B-V)$ (1)	σ (2)	V (3)	n (4)	$\sigma(B-V)$ (5)	$\eta(B-V)$ (6)
... .	...	21.5	...	0.00	0.02
0.005	0.079	22.0	4	0.02	0.03
0.010	0.075	22.5	10	0.06	0.04
−0.017	0.128	23.0	9	0.08	0.08
0.091	0.163	23.5	18	0.14	0.10
... .	...	24.0	...	0.30	0.15

data. In Table 6 column (1) gives the mean color difference between the recovered and inserted star and column (2) the standard deviation, both as a function of V magnitude (col. [3]). These results show that there is no significant measuring bias[3] brighter than $V=23.5$, where we see a 2 σ error in the sense that the measured stars are redder than the inserted stars.

This experiment also offers us a more comprehensive measure of the photometric errors. The standard deviations in column (2) include the effect of source confusion in addition to the DC level of sky background. These estimates may be compared with the mean range in $B-V$ measurements for the 122 stars measured twice (col. [5]) and 1 σ errors calculations from photon statistics (star and sky) given in column (6). Since the error sources here are not independent, we have simply taken the maximum value at any given magnitude to represent the color uncertainties in Figure 2. The uncertainties in V magnitudes were estimated similarly. Note that this yields a 1 σ uncertainty of 0.13 mag in $B-V$ at $V=23.0$. The 1 σ width (rejecting 3 σ deviates) of the color-magnitude diagram at that magnitude is also 0.13. We conclude that any intrinsic dispersion in the color of the Carina main-sequence turnoff is below the level of detection in the present data.

[3]Compare col. [1] with $\sigma/\sqrt{n}$.

IV. COMPARISON WITH GLOBULAR CLUSTERS AND ISOCHRONES

The interstellar extinction to Carina is $E(B-V)=0.025\pm0.01$ according to the reddening map of Burstein and Heiles (1982) and Burstein (1983, private communication). Direct comparison of the color magnitude diagram can therefore be made with the Draco dwarf spheroidal and the globular cluster M92. In particular (all other things being equal), the similarity of the color of the giant branch at the HB level (cf. Stetson 1981) would indicate that the metallicity of Carina would be comparable to that of Draco, which in turn equals *in the mean* that of M92 (Kinman, Kraft, and Suntzeff 1980).

The analogy with M92 is strongly violated, however, at the main-sequence turnoff. Figure 2 shows the ridge line of the M92 color magnitude diagram by Sandage (1970) shifted fainter by $\delta(m-M)=5.4$ so as to superpose the HB V magnitudes. Because of its low metallicity, M92 has the bluest and brightest turnoff of a set of coeval Galactic globular clusters. Yet the Carina turnoff is much bluer and brighter than M92, which indicates a younger age.

A simple way to estimate the age difference between Carina and M92 uses the magnitude difference between the turnoff and the HB, following the parameterization by Sandage (1982). We can use his equations (1), (14a), and (15a) to do this, provided we take account of the small effect on $(B-V)_{0,g}$ of the age difference. Adopting $V=23.0 \pm 0.2$ for the Carina turnoff, and $\delta(\mathrm{BC}) = 0 \pm 0.05$ for the bolometric correction difference between Carina turnoff and (hypothetical) RR Lyrae stars (see Rabin 1981), we rapidly converge on values of 7 ± 1 Gyrs for the age and -1.9 ± 0.2 for [Fe/H].

Isochrones interpolated from the data given by Ciardullo and Demarque (1979) are also shown on Figure 2 for ages of 6 and 9 Gyrs at this metallicity (and $Y=0.2$). If a single age is to represent the data, a 6 or 7 Gyr isochrone would seem the most appropriate although, given the size of the uncertainties in $B-V$, a formal fitting procedure like that of Johnson and Flannery (1981) would be required to produce a quantitative answer. We have refrained from doing this, however, because of the clear presence of "blue stragglers" above the main-sequence turnoff, which would bias an attempt to fit a single-age model. Further discussion on this subject follows in the context of the Carina luminosity function.

Finally, we note that within the limits of the handful of HB stars visible in this field and the presence of one or two foreground stars in this region of the color-magnitude diagram, no extension of the HB into the instability strip was noted, nor do we have any candidates for HB or supra-HB variable stars.

TABLE 7

CARINA LUMINOSITY FUNCTION

M_v (mag) (1)	Number $< M_v$ (2)	Control Field (3)	log Φ (4)
0.3	5	0	
0.5	16	2	
0.7	44	2	
0.9	50	3	
1.1	59	4	
1.3	62	5	
1.5	73	5	
1.7	81	6	
1.9	88	6	0.85
2.1	98	7	1.20
2.3	127	8	1.64
2.5	154	11	1.83
2.7	189	12	2.01
2.9	286	12	2.30
3.1	346	16	2.41
3.3	450	21	2.55
3.5	535	26	2.64
3.7	635	30	2.72
3.9	775	32	2.82
4.1	899	32	2.90

V. THE LUMINOSITY FUNCTION

The area over which photometry has been carried out in the composite Carina field is almost identical to the area of the control field. So it is a straightforward matter to construct an apparent luminosity function from the data in Tables 4 and 5. To simplify comparison with models we chose to begin at the HB (assumed[4] to have $M_v = 0.6$), and it was therefore possible to exclude all stars with $B-V > 1.0$.

Estimate of the true luminosity function, however, requires a completeness correction. This was determined by means of the artificial starfield experiment described in the previous section. The luminosity function of the added stars was known by construction. And care was taken to select artificial stars for photometry with the same criteria used for real stars. So the completeness correction could be obtained as the ratio of recovered to added stars. This method will be accurate as long as the confusion is not materially increased by the addition of stars.

Determination of the Carina luminosity function is detailed in Table 7. The number of stars brighter than M_v (and fainter than $M_v = 0.1$) is indicated in column (2) for Carina (after correction for incompleteness), and in column (3) for the control field. The control field was not corrected for incompleteness, as the effects of crowding are negligible. A check on this was available through a comparison of stars[5] between $V=20$ and 22 with $B-V>1$ in the two fields.

The difference between the fields is listed in column (4) starting $(\Phi = 0)$ at $M_v = 1.7$. These values are plotted in Figure 4 together with theoretical (cumulative) luminosity functions calculated by Ciardullo and Demarque (1976) for two choices of the initial mass function. Bolometric corrections were taken from Rabin (1981). Within the uncertainties, which are principally due at the faint end to the completeness corrections, the 7 Gyr luminosity function is an acceptable fit to the data. If multicomponent models are to be contemplated, the fit could be improved by the addition of somewhat younger stars. Indeed there is evidence in the color-magnitude diagram for such stars (unless we suppose that the blue stragglers are binaries). But the addition of a large old population (16 Gyrs) would lead to a steeper

[4]The correction for a younger HB is not significant (Sandage 1982, equation A5).

[5]A comparison with the statistics of faint objects by Tyson and Jarvis (1979) suggests that many of these "stars" may be background galaxies.

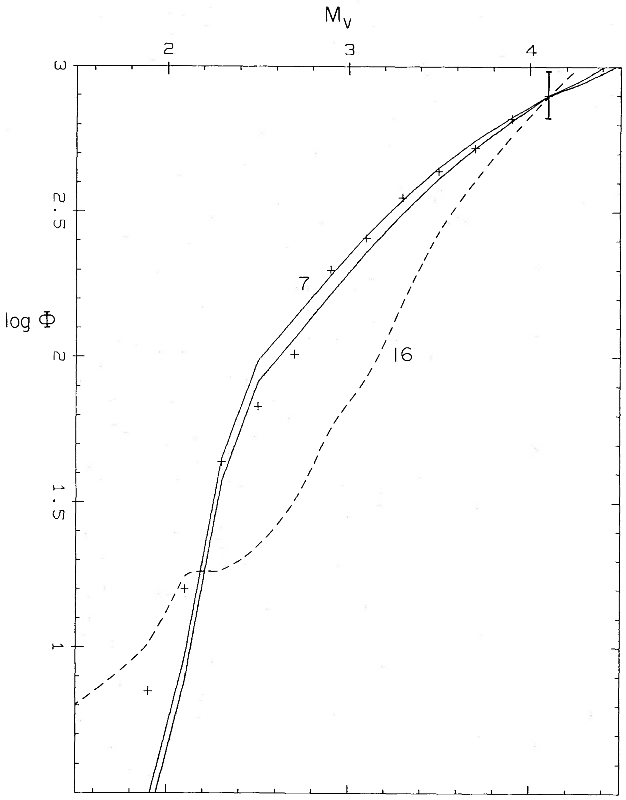

FIG. 4.—The cumulative luminosity function from $M_v = 1.7$ to 4.1 in Carina. The data (*crosses*) are well fitted by theoretical luminosity functions due to Ciardullo and Demarque, normalized to the same total number of stars. The two solid lines have ages of 7 Gyrs and power law initial mass functions of Ciardullo and Demarque slope parameter $s = 0$ and $s = 2.35$. The dashed line has age 16 Gyrs, and applies to both s values. All three theoretical relations have $Y = 0.2$ and $Z = 0.0001$.

model luminosity function and a worse fit. Of course, we cannot rule out the existence of a small minority old population. But the best fit to the current data implies that the bulk of the Carina dwarf is of intermediate age.

VI. SUMMARY

Our results can be summarized as follows:

1. The Carina dwarf in spite of its low luminosity and metallicity has a well-defined, red horizontal branch at $V = 20.5$ mag. With $E(B - V) = 0.025$ and $M_{v,\mathrm{HB}} = 0.6$, a reddening corrected distance modulus $(m - M)_0 = 19.8$ mag results. The Ursa Minor dwarf remains the only dwarf spheroidal in the remote halo which does not have a red horizontal branch.

2. Sandage's $(B - V)_{0,g}$ calibration yields an estimate for Carina's metallicity of $[\mathrm{Fe/H}] = -1.9 \pm 0.2$. The sparsely populated giant branch does not allow any estimate of the possible metallicity range to be made, although the narrowness of the giant and subgiant branch near the horizontal branch suggests that such a range is not large (cf. Cannon and Stewart 1981, Fig. 2). Spectroscopic investigation into this subject would be of interest.

3. Both isochrone fitting and the horizontal-branch, turnoff separation $\Delta M_{\mathrm{HB-TO}} \sim 2.5$ suggest an age for Carina between 6 and 9 Gyr. A more quantitative age estimate is hindered by the apparent presence of a significant blue straggler population. It remains uncertain both in this context and in general whether blue stragglers in old populations are young stars or binaries.

4. Comparison with the theoretical luminosity functions of Ciardullo and Demarque suggests that the number of stars as old as galactic globular cluster stars in Carina is small and possibly zero. Further support for this latter conclusion comes from the fact that there are as many carbon stars in Carina per unit luminosity as there are in intermediate-age globular clusters in the Magellanic Clouds (see Mould *et al.* 1982).

It is interesting, finally, to note that the emerging picture from main-sequence photometry of the dwarf spheroidals is of an age *spread* in the outer halo (cf. Da Costa and Mould 1983), consistent with the ideas of Zinn (1978). These results continue to challenge our understanding of the formation of dwarf elliptical galaxies.

It is a pleasure to express our appreciation of the efforts of all those responsible for creating the 4 m prime focus CCD camera system, one of the finest instruments built by AURA, in our opinion. Special thanks go to Harvey Butcher and Pat Seitzer. We are also grateful to Arlo Landolt for providing results ahead of publication and Jerome Kristian, Keith Shortridge, and Ramon Galvez for help with software. This work was partially supported with funds from NSF grant AST81-17365.

REFERENCES

Aaronson, M., Olszewski, E. W., and Hodge, P. W. 1983, *Ap. J.*, **267**, 271.
Adams, M., Christian, C., Mould J., Stryker, L. and Tody, D. 1980, *Stellar Magnitudes from Digital Pictures* (Tucson: Kitt Peak National Observatory).
Burstein, D., and Heiles, C. 1982, *A.J.*, **87**, 1165.
Cannon, R. D., Demers, S., Hawkins, M. R. S., Kunkel, W., and Pritchet, C. 1983, in preparation.
Cannon, R. D., Hawarden, T. G., and Tritton, S. B. 1977, *M.N.R.A.S.*, **180**, 81P.
Cannon, R. D., Niss, B., and Norgaard-Nielsen, H. U. 1981, *M.N.R.A.S.*, **196**, 1P.

Cannon, R. D., and Stewart, N. H. 1981, *M.N.R.A.S.*, **195**, 15.
Ciardullo, R. B., and Demarque, P. 1976, *Trans. Yale Obs.*, Vols. **33–35**.
______. 1979, *Dudley Obs. Rept.*, **14**, 317.
Da Costa, G. S., and Mould, J. R. 1983, in preparation.
Graham, J. A. 1981, *Pub. A.S.P.*, **93**, 29.
______. 1982, *Pub. A.S.P.*, **94**, 244.
Johnson, B. C., and Flannery, B. P. 1981, *Bull. AAS*, **13**, 871.
Kinman, T. D., Kraft, R. P., and Suntzeff, N. B. 1980, in *Second Workshop on Physical Processes in Red Giants*, ed. A. Renzini, I. Iben, Jr. (Dordrecht: Reidel), p. 71.
Mould, J. R., 1982, Highlights of Astronomy, **6**, in press.
Mould, J. R., Cannon, R. D., Aaronson, M., and Frogel, J. A. 1982, *Ap. J.*, **254**, 500.
Rabin, D. 1981, Ph.D. thesis, California Institute of Technology.
Sandage, A. R., 1970, *Ap. J.*, **162**, 841.
______. 1982, *Ap. J.*, **252**, 553.
Seitzer, P., Da Costa, G. S., and Mould, J. R. 1983, in preparation.
Stetson, P. B. 1981, *A.J.*, **85**, 387.
Tyson, J. A., and Jarvis, J. F. 1979, *Ap. J. (Letters)*, **230**, L153.
Zinn, R. 1978, in *Globular Clusters*, ed. D. Hanes, and B. Madore (Cambridge: Cambridge University Press), p. 191.

MARC AARONSON: Steward Observatory, University of Arizona, Tucson, AZ 85721

JEREMY MOULD: Caltech 105-24, Pasadena, CA 91125

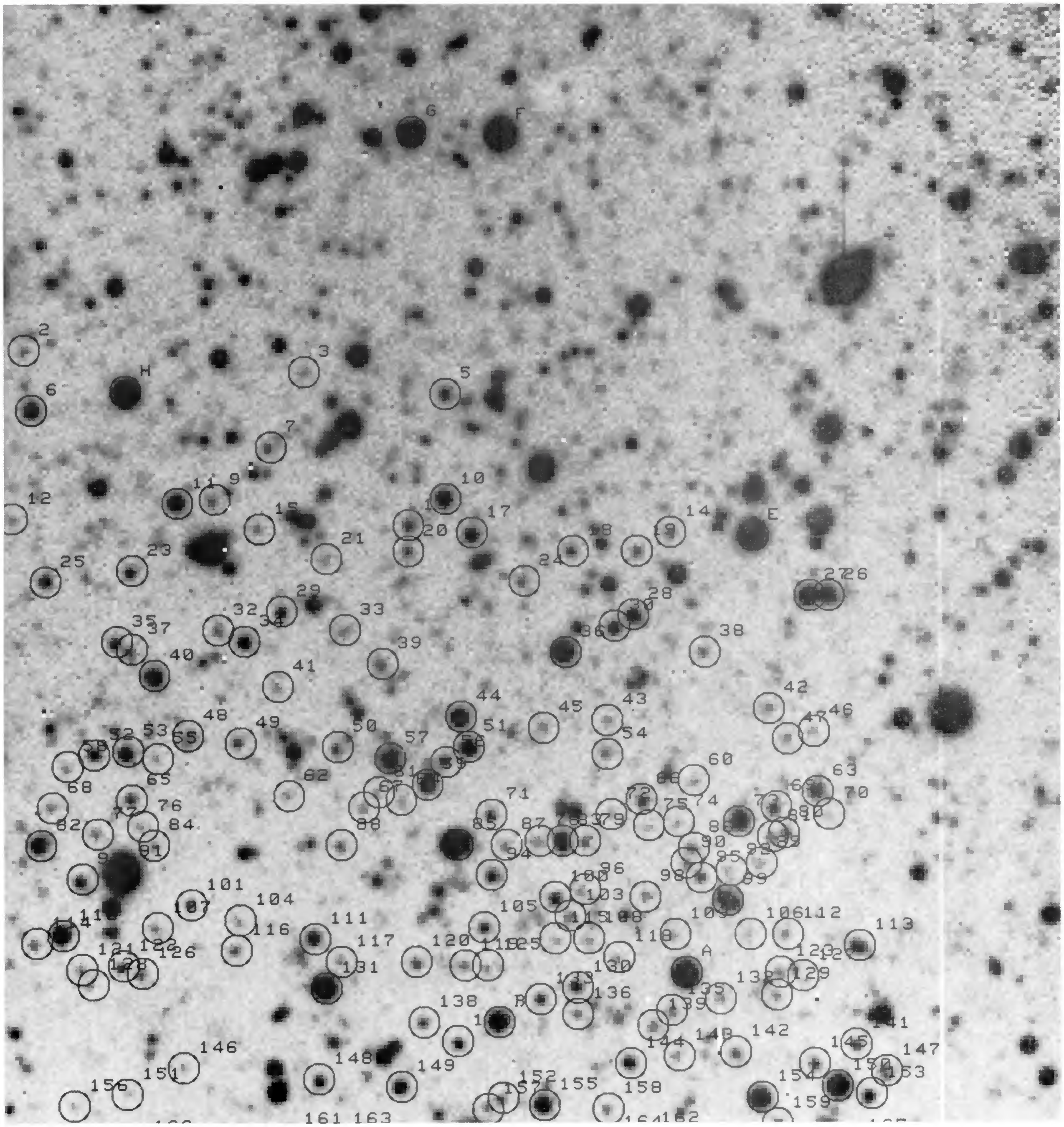

FIG. 1*a*

FIG. 1.—Identification charts are shown for (*a*) the Carina 1 field, (*b*) the Carina 2 field; and (*c*) the Carina control field. Secondary standards from Tables 2 and 3 are labeled with letters, while program objects from Tables 4 and 5 are labeled by number.

MOULD AND AARONSON (*see* page 531)

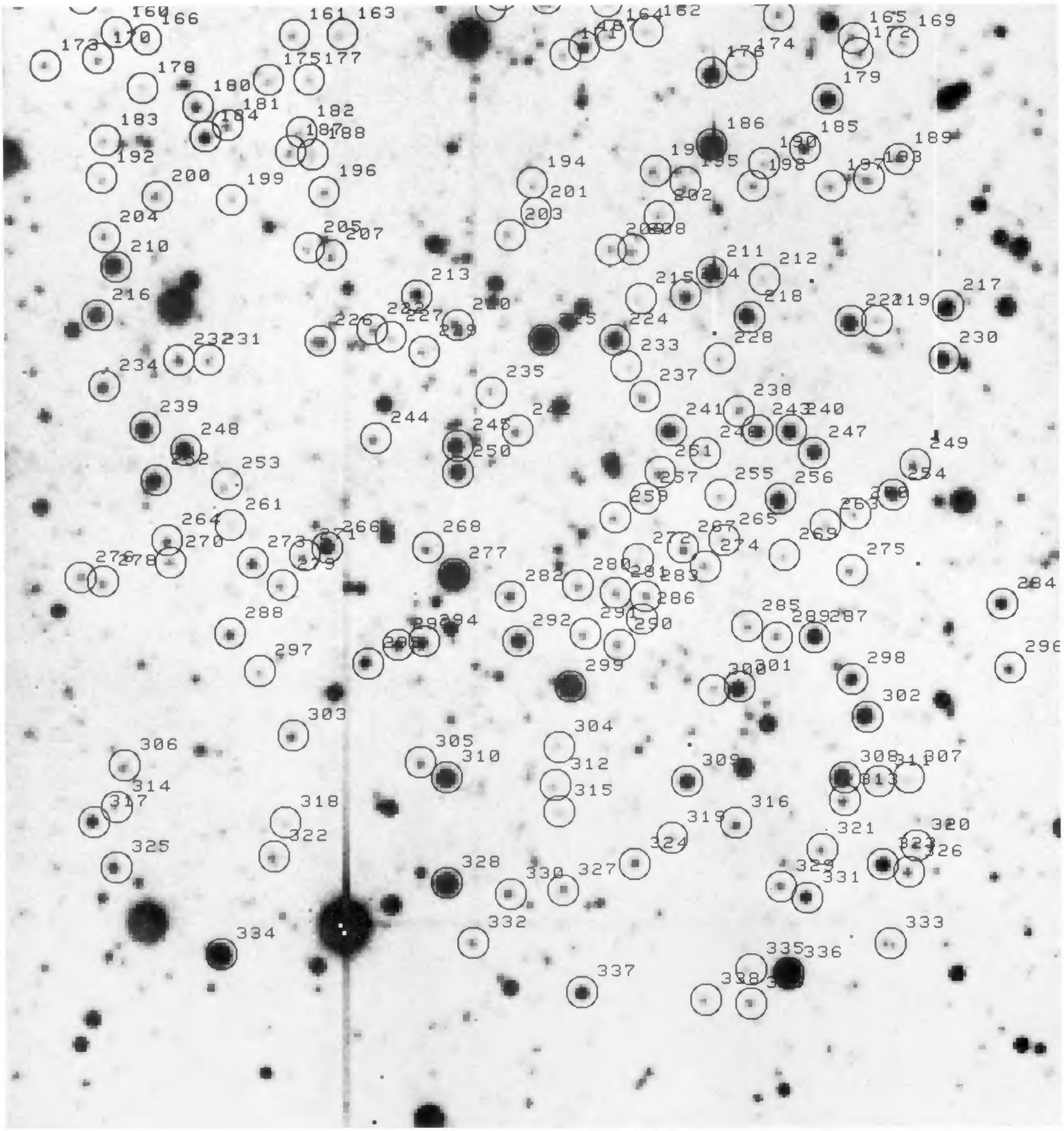

FIG. 1*b*

MOULD AND AARONSON (*see* page 531)

PLATE 28

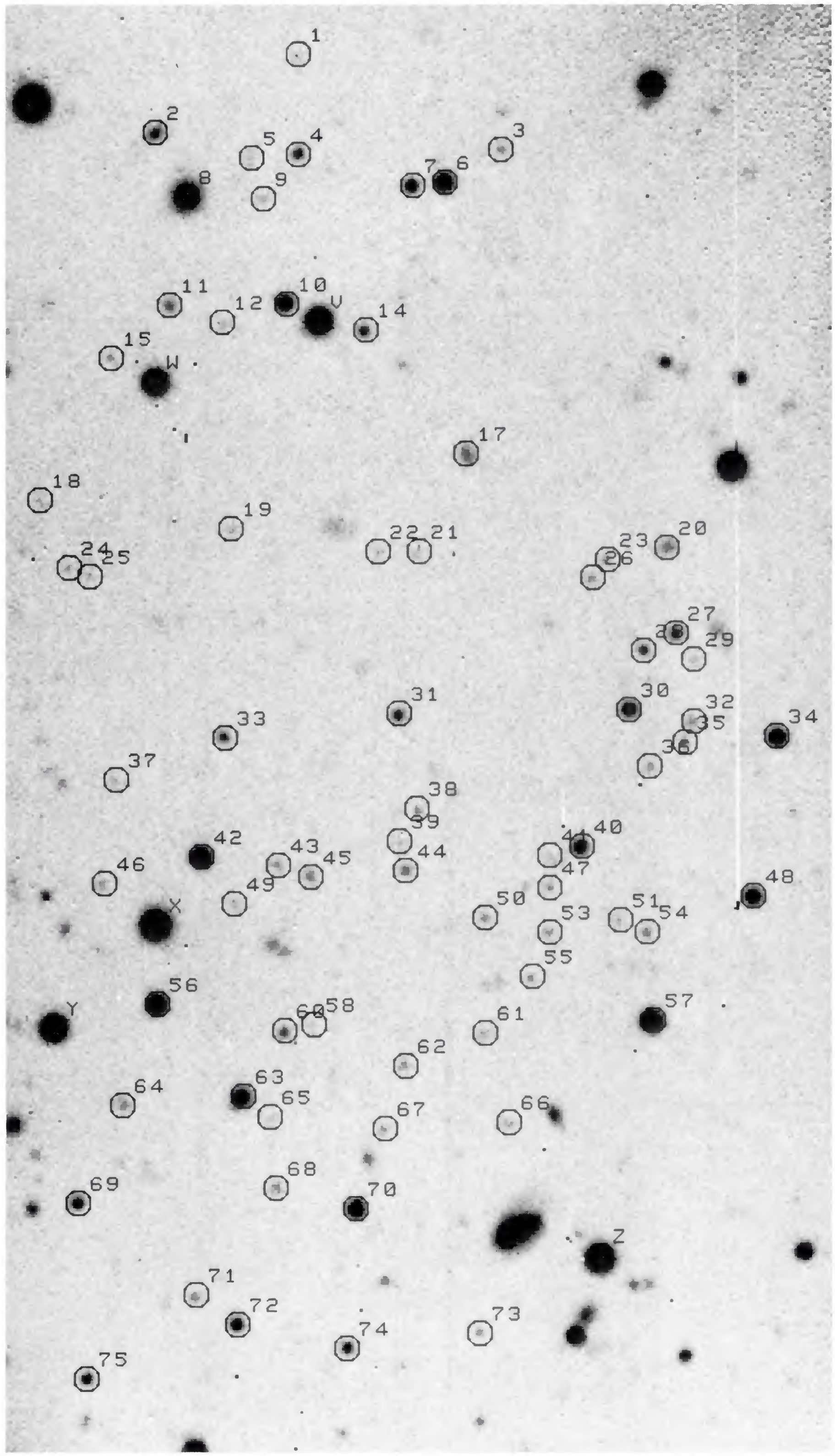

FIG. 1*c*

MOULD AND AARONSON (*see* page 531)